April 8, 2025

We wish to thank the reviewer for their helpful and constructive comments. The reviewer's comments and questions are addressed below.

Reviewer 2

The manuscript by Yalla et al analyzes different AWM strategies by using SPOD to isolate different modes in the flow at different frequencies related to the AWM excitation frequency. The work has significant scientific value as it furthers our understanding of the flow dynamics associated with AWM. On the other hand, the current manuscript leaves some room for improvement in terms of structure, and some of the results presented require additional analysis or explanation. In short, I feel like this manuscript is a very rough diamond. It should in my opinion be published after the authors perform some serious polishing. I voted to accept subject to minor revisions, because I believe in the value of this manuscript, but please note that some of the changes I feel are necessary are leaning towards "major revisions".

Major Comments

1. You mention in the second line of the introduction that power losses are particularly problematic in stable ABL, most commonly found in offshore wind farms. Yet, in section 2.1, you derive the simulations from measurements from an onshore farm. Please explain or justify why you did not choose to run simulations to match offshore conditions, where AWM would be expected to be most effective.

   Wake mixing strategies are most beneficial in stable ABLs with low TI, where wakes are known to persist far downstream of turbines. While stable ABLs are indeed common offshore, they also occur in onshore environments. Consider, for example, the histograms in Figure 1, which show wind speed and turbulence intensity measurements taken offshore at the NY Bight and onshore measurements taken as part of the AWAKEN campaign. Both cases exhibit low TI, region 2 wind speeds that are representative of stable ABL conditions and are conducive to wake mixing strategies.

   The decision to utilize measurements from the AWAKEN domain was, in part, driven by funding logistics and project scope; however, the authors are confident that the AWAKEN measurement still lead to valid stable conditions, especially for the 1,100-seconds needed for the simulations in this study.

   To avoid any potential confusion regarding the context of our simulations, we have revised the introduction to remove the specific mention of offshore conditions.

2. Similarly, the choice of wind speeds, wind directions, TI's, and veer that is studied needs more justification. I can see how these conditions would correspond to a stable ABL, but I don't see how these specific conditions are necessarily prerequisites for a stable ABL. Is there literature available describing ABL's in the AWAKEN experiment that supports this choice? Or are there other reasons you have chosen these conditions specifically? Also, please define the definition of wind direction and why these directions are more likely to result in stable ABL's than other WD's. Furthermore, please clarify whether the 230 minute dataset used is continuous or a combination of different subsets. Finally, in line 102, you mention that the resulting veer is 9 degrees, which is

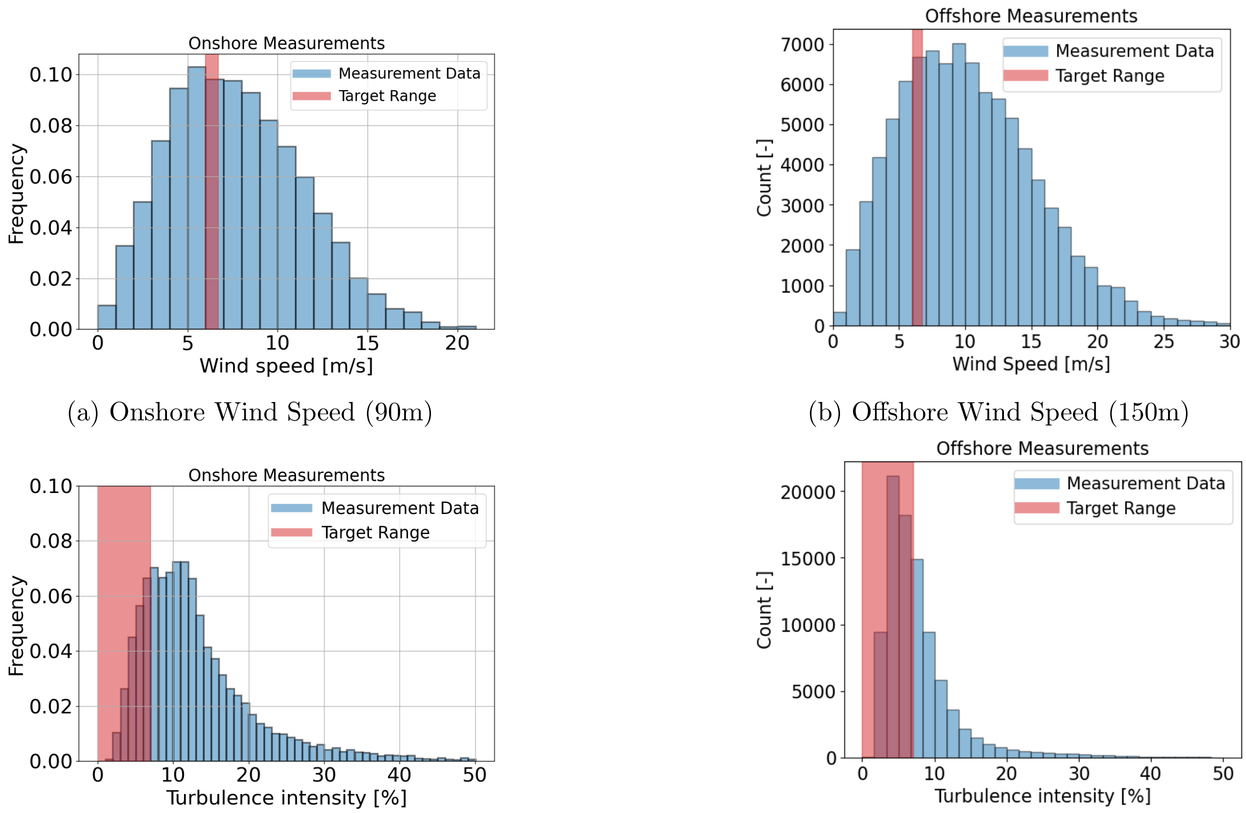

(a) Onshore Wind Speed (90m)

(b) Offshore Wind Speed (150m)

(c) Onshore TI (60m)

(d) Offshore TI (150m)

Figure 1: Comparison of wind speed and TI measurements taken at onshore as part of the AWAKEN campaign and offshore at the NY Bight

substantially lower than the threshold you mention earlier. Please explain why this is the case and how this still accurately represents the dataset, as we have seen in recent publications by Brown et al (2025) and Frederik et al (2025) that lower veer can have a large impact on how well different AWM strategies work.

The authors agree that insufficient information was provided in the original manuscript regarding the target wind conditions and their derivation from a field campaign. The text has been rewritten to improve clarity and accuracy. We believe the reviewer's questions are answered directly by the new text (in **bold**):

The streamwise and lateral boundary conditions are defined by an inflow condition extracted from an initial precursor simulation. The target conditions for the precursor simulation are derived from stable ABL measurements taken in 2021 concurrent with the American Wake Experiment (AWAKEN) campaign (Moriarty et al., 2024). Specifically, the atmosphere was sampled at the Department of Energy's Atmospheric Radiation Measurement (ARM) Southern Great Plains (SGP) C1 site **using a Doppler profiling lidar and CO_2 flux stations. A number of filters were applied to isolate 30-minute bins corresponding to high-quality measurements and periods of likely interest for wake control. Balancing the need for appreciable sample size with that for retaining the realism**

of a specific, observable ABL condition, the latter filters isolated a wind condition with a frequency of occurrence: wind speed between 6 and 6.7 m/s, wind direction ranging from 100° to 260° (assuming a clockwise definition of wind direction with 0° corresponding to northerly flow), and turbulence intensity (TI) from 0% to 7%. The 1200 minutes of (non-contiguous) data that meet the above criteria are used to establish target statistics for the precursor simulation, and these are a hub-height wind speed of 6.4 m/s, a TI of 4.4%, a shear exponent of 0.19, and 17° of veer over the height of the rotor disk. The low TI and high veer in this target are congruent with the southerly, stable ABL conditions typically observed at the SGP site (Krishnamurthy, 2021), and these conditions offer a strong opportunity to demonstrate a use-case for wake-control technology.

The surface roughness height (0.0015 m) and cooling rate (4.16×10^{-5} K/s) parameters are calibrated in the precursor simulation of the ABL to ensure good agreement between the simulated and measured flow statistics; this calibration results in inflow data with an average hub-height wind speed of $U_{\text{inf}} = 6.4$m/s, a TI of 3.5%, a shear exponent of 0.17, and 9° of veer over the height of the rotor disk. Notably, the simulated ABL exhibits less veer than the measurement data, and this is due to the numerical forcing scheme used to drive the ABL towards the target statistics (primarily TI and shear), which limits the amount of simulated veer that can be achieved while maintaining a realistic ABL velocity profile (note that such difficulty achieving high veer was also encountered in Brown et al. (2025) and Frederik et al. (2025)). Alternate ABL forcing schemes, such as those which incorporate meso-scale information in a direct assimilation approach, may be able to match the veer and wind speed profiles, but are not studied here. In addition to the above summary statistics, comparisons of the vertical profiles between the simulated and measured ABL condition are found favorable (see Figure 3).

3. I agree with Reviewer 1 that not all figures add value to the paper. Consider removing Figure 2, 4 (unless you add the Cp/Ct curves of the turbines in the actual WF for comparison), 7, 21, and 22. Furthermore, I would be interested to also see a comparison between data and simulation in the time and/or frequency domain in Figure 3, not just a comparison of averages.

   The authors have removed Figure 2 from the original manuscript and thank the reviewer for this suggestion. The other figures have been retained. See below for additional comments regarding figures 7, 21, and 22. In the current study, the most meaningful comparisons between the simulated and measured ABL data would be of the 10-min averaged statistics, both in terms of the vertical velocity profiles and the hub-height quantities such as shear, turbulence intensity, and wind speed. Because the precursor development used constant surface roughness, surface temperature properties, and target wind speed/direction during the spin-up phase, the time evolution of the ABL leading up to the simulation period is not expected to match the same behavior as the measured data. In other ABL forcing schemes, such as approaches which use meso/micro-scale coupling, a direct comparison of the ABL properties is more meaningful. Such forcing schemes are under active development and are planned for use in future work. We have clarified the information regarding the measurement data and the formulation of the precursor in the manuscript.

4. I have concerns about the azimuth angle approximation stated on line 151-153. I have seen simulations in similar wind conditions, and especially if you are implementing AWM, I would expect non-negligible changes in rotor speed. Even tiny changes could affect the outcome of your Fourier approximation as you are in practice taking the transformation of a mode/azimuthal wave frequency that is variable over time. I would like to see what effect these variations have on the Fourier transformation, i.e., how well of an approximation Eq.(3) is w.r.t. Eq.(2). In fact, my guess would be that most of the non-periodicity that you describe in line 156 is caused by this fluctuation in rotor speed, not by the non-uniform inflow. Have you checked the periodicity when you don't use the rotor speed approximation? How wide is your window now? I believe the rotor speed approximation might be reasonable to make in combination with a windowed transform, but would like to see this better studied or more accurately described in this section.

   The authors thank the reviewer for their suggestion to re-examine the formulation of the blade-loading spectra. Although the mean-rotor speed approximation provides a convenient way of translating timeseries data from OpenFAST to spectra using a single Fourier-transform, it is not strictly necessary. Moreover, it may not be exact due to fluctuations in the rotor speed, as the reviewer points out. To address this, the authors have developed an alternative method for the computing the spectra by forming $F_x(r, \theta, t)$ directly using the instantaneous rotor speed signal to inform the azimuthal position of the turbine blade. Consequently, the spectra of the axial blade force at a particular azimuthal wavenumber, κ_θ, and frequency, ω, can be computed by performing a Fourier-transform in both the azimuthal and temporal directions, i.e.,

$$\hat{F}_x(r, \kappa_\theta, \omega) = \int \int F_x(r, \theta, t) e^{-i(\omega t + \kappa_\theta \theta)} d\theta dt.. \tag{1}$$

   The updated results using this formulation are shown in Figure 2 of this document and have been included in the manuscript. No major differences with the original formulation are observed, and the main results and conclusions of this section are unchanged.

5. In Section 3.1, I would be very interested to see an analysis of the eigenvalues of the baseline case for different values of St. The main hypothesis of why St=0.3 is optimal, is that it excites natural modes in the flow. Therefore, I would expect that taking the Fourier transform at different frequencies would result in lower values. Adding an analysis of the magnitude of different wavenumbers as a function of Strouhal numbers (say St=0.1 to 0.6) could reinforce or disprove this hypothesis and thus add significant value to the scientific contribution of this paper.

   The authors appreciate the reviewer's interest in the eigenvalues of different Strouhal numbers for the baseline case. These results are shown in Figure 3 of this document. It is generally observed that the eigenvalues at $St = 0.3$ are larger than the other Strouhal numbers, although there is some variability depending on the azimuthal wavenumber and streamwise location.

   The authors would like to clarify that the manuscript does not claim that $St = 0.3$ is necessarily the optimal choice, but rather highlights that the performance of AWM strategies when forced at $St = 0.3$ corresponds to their ability to excite natural modes in the flow at this Strouhal number. The value of $St = 0.3$ was chosen based on recommendations in the literature, where it is generally found that Strouhal numbers between 0.2 and 0.35 perform well. However, the optimal value is still an open question. The SPOD parameters in this study were chosen to maximize the number of "blocks" over the 1,100s time interval while ensuring good temporal resolution of the forcing Strouhal number $St = 0.3$. As such, there is

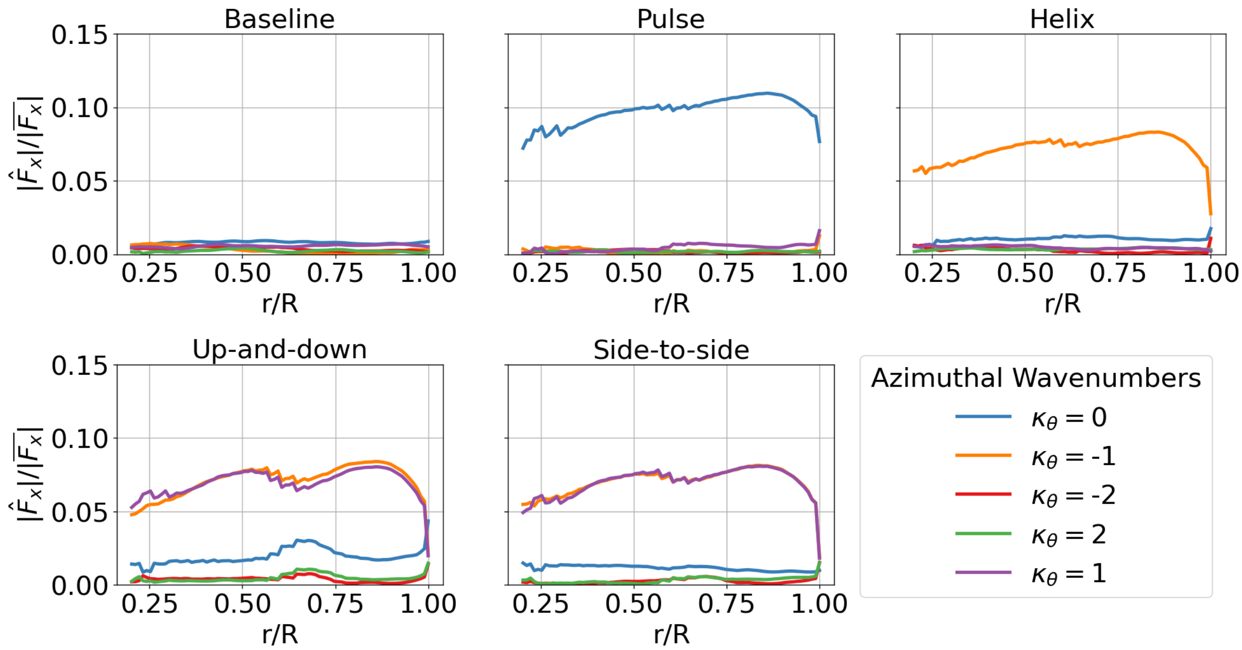

Figure 2: Variations in the axial blade loading for each AWM strategy. The individual curves correspond to the magnitude of the Fourier coefficients of the axial force, $|\hat{F}_x|$, at $St = 0.3$ for different azimuthal wavenumbers, κ_θ, normalized by the mean axial blade loading, $|\overline{F}_x|$.

insufficient resolution to do a refined SPOD study of the baseline wake for different Strouhal numbers between 0.2 and 0.35. Since the eigenvalues of the baseline at $St = 0.3$ are extensively shown throughout the manuscript, the authors have decided not to include Figure 3 of this document in the final version. However, this type of analysis will be considered for future studies that consider the optimal choice of forcing frequency.

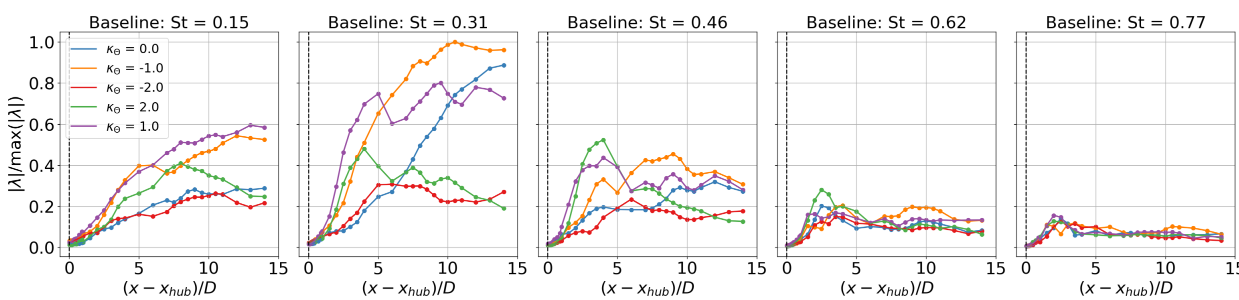

Figure 3: SPOD eigenvalues for the baseline wake at five different Strouhal numbers

6. I suggest restructuring Section 3.1 and its figures, as it is very hard to follow now. I keep having to scroll through pages to get to the figures that are covered in the text. For example, perhaps you should redo figures 9 and 10 so one of them shows the global EVs for both ranges, and the other the baseline-normalized EVs, as this is also how it's discussed in the text. Similarly, perhaps put fig 11a and 12 together for better comparison. All the other panels of fig 11 don't seem to be discussed, but could probably do with some more explanation as these results are probably

interesting but not self-explanatory. In general, I would restructure this section so the analysis is grouped in the same order as the figures. That way, the reader no longer needs to scroll back and forth between pages every couple of lines. I would also consider splitting this subsection into multiple (sub)subsections to better separate different points that you are trying to make.

The authors appreciate the reviewer's constructive feedback regarding the structure of Section 3.1 and the associated figures. We have restructured Figures 9 and 10 in the original manuscript to align with the reviewer's suggestion. The baseline-normalized eigenvalues are now shown together in one figure, with the top row corresponding to the near-turbine region, $-1 \leq (x - x_{hub})/D \leq 1$, and the bottom row corresponding to the entire streamwise domain, $-5 \leq (x - x_{hub})/D \leq 14$ (see Figure 5 in this document). Likewise, the globally-normalized eigenvalues are also shown together in one figure using the same layout (see Figure 4 in this document). We feel this better aligns the figures with the order the analysis. Regarding the reviewer's second comment, the authors have decided to keep Figures 11a-d in the original manuscript together to illustrate the progression of the dominant SPOD modes through the wake, and have added additional clarifications for panels b-d of this figure. The phase-averaged, baseline-subtracted velocity fields are included on the page immediately following the figure of SPOD modes to hopefully minimize page turning by the reader for this comparison. Furthermore, the authors will do their best to position the figures as close to the locations where they are discussed in the paper, and will work with the journal's editorial team to correct the typesetting and placement of figures in the final version of the manuscript.

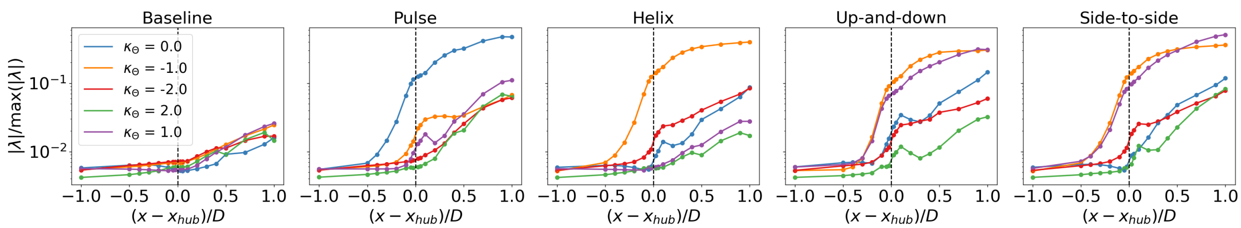

(a): Globally-normalized eigenvalues of $\boldsymbol{S}$ at $St = 0.3$ for $-1 \leq (x - x_{hub})/D \leq 1$

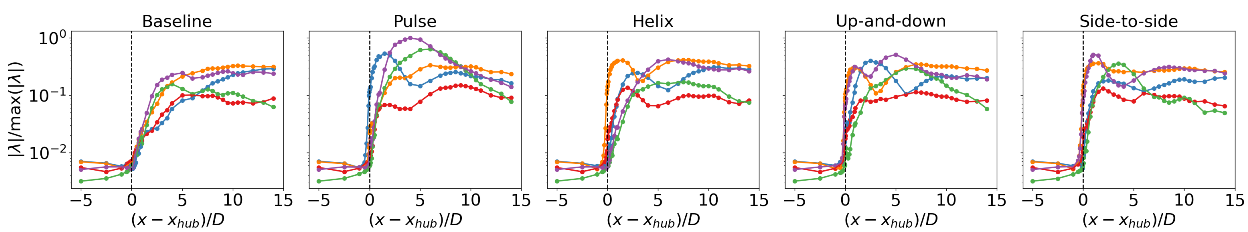

(b): Globally-normalized eigenvalues of $\boldsymbol{S}$ at $St = 0.3$ for $-5 \leq (x - x_{hub})/D \leq 14$

Figure 4: Eigenvalues of $\mathbf{S}$ at $St = 0.3$ for the azimuthal wavenumbers $wkappa_\theta = 0$ (—), $\kappa_\theta = 1$ (—), $\kappa_\theta = -1$ (—), $\kappa_\theta = 2$ (—), and $\kappa_\theta = -2$ (—). Each eigenvalue is normalized by the global maximum eigenvalue across all AWM cases and streamwise locations.

7. I question the fidelity of the results presented in Figure 23 and surrounding text. The different pitch amplitude cases raise more questions to me than they answer. First, the upstream power gain at low amplitudes is very peculiar and should be studied. Same goes for the fact that helix and up-down lose downstream power when the amplitude increases. These results make me question

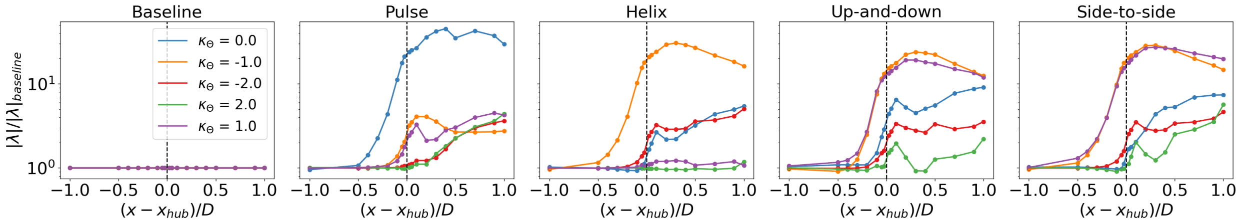

(a): Baseline-normalized eigenvalues of $\boldsymbol{S}$ at $St = 0.3$ for $-1 \leq (x - x_{hub})/D \leq 1$

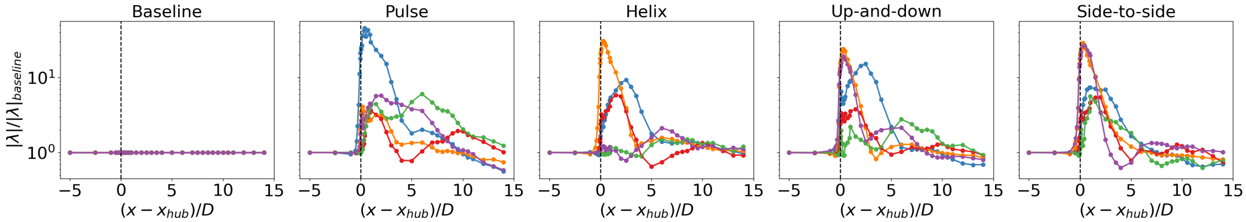

(b): Baseline-normalized eigenvalues of $\boldsymbol{S}$ at $St = 0.3$ for $-5 \leq (x - x_{hub})/D \leq 14$

Figure 5: Eigenvalues of $\mathbf{S}$ at $St = 0.3$ for the azimuthal wavenumbers $wkappa_\theta = 0$ (—), $\kappa_\theta = 1$ (—), $\kappa_\theta = -1$ (—), $\kappa_\theta = 2$ (—), and $\kappa_\theta = -2$ (—). The eigenvalues for each wavenumber and streamwise location are normalized by the corresponding eigenvalues in the baseline case.

the fidelity of the standalone OpenFAST model approach used, as the results do not align with similar studies performed using higher fidelity tools. I think you need to choose to either remove this analysis from the paper, or dive in deeper to explain why these results are different from literature. I recommend doing the former, as this analysis does not align with the main findings of the paper to begin with. Same can be said about Figure 24.

Upon further investigation, an error was identified in the computation of the statistics for the two-turbine array. This led to the two errors pointed out by the reviewer: an artificial increase in the power of the upstream turbine at $A = 0.5°$ and a decrease in the downstream turbine's power with pitch amplitude for certain cases. In the original results, time-series data was averaged over different time intervals between each AWM case and the baseline case, leading to inconsistent comparisons of power. In the updated results (Figure 6), the averaging interval has been fixed so that all cases, including the baseline, are averaged over an even number of Strouhal periods. As a result, there is no longer a significant increase in the power of the upstream turbine at $A = 0.5°$. Moreover, the power of the downstream turbine now increases with pitching amplitude for all forcing strategies, as the reviewer expected to see.

To strengthen the connection between these results and those in the previous section we have also included the results for the downstream turbine's power as a function of streamwise spacing, rather than solely presenting the combined power of the two-turbine array. These trends align well with the rotor-averaged velocities presented earlier in the manuscript. See the responses to the minor comments below for a further discussion of the setup used to generate these results.

We greatly appreciate the reviewer's suggestion to re-examine these results, which has led to

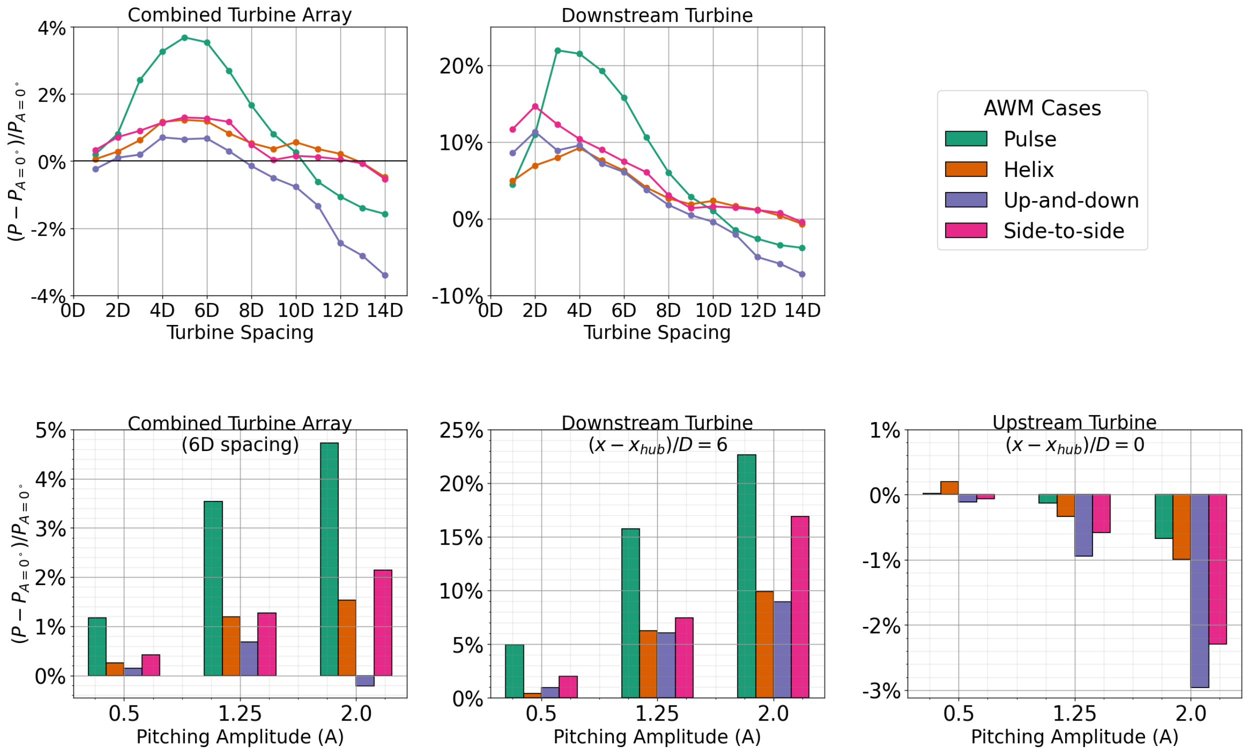

Figure 6: (top) Percent change in generated power, P, from the baseline case ($A = 0°$) for a two turbine array with the turbine spacings ranging from $1D$ to $14D$. AWM is applied to the upstream turbine with $A = 1.25°$, while the downstream turbine is operated using baseline controls. (bottom) Percent change in generated power from the baseline case for the two turbine array with $6D$ spacing for three different pitching amplitudes applied to the upstream turbine, $A = 0.5°$, $A = 1.25°$, and $A = 2.0°$. Results for the combined two turbine array, the upstream turbine, and the downstream turbine are shown.

these important clarifications.

Minor Comments

The authors have done their best to address all minor issues raised by the reviewer. These suggestions were helpful in improving the clarity of the manuscript. Further responses to a selection of the reviewer comments are included below.

- Line 56-57: I agree with the first reviewer that Muscari et al, 2022 and/or 2025, and/or Gutknecht et al, 2023 should be cited and discussed here, or in line 61-62. It seems to me that these studies use a slightly different method to achieve a similar goal. It would therefore be worthwhile to discuss the differences between and/or advantages and disadvantages of both methods.

  Thank you for the relevant references — citations have been added to the manuscript.

- Line 123: This equation is not self-explanatory. Although I can see the value of this definition in light of the SPOD modes later on, I feel like this definition of the blade pitching is far less intuitive than the one used in publications by other groups, that uses the MBC/Coleman transformation.

Consider relating this equation to that definition, or at least adding blade number subscripts and explaining what the definition of the clocking angle is.

The authors have retained the normal-mode formulation of the blade-pitch because it aligns directly with the azimuthal and temporal frequencies that are analyzed through the SPOD analysis. This justification for using the normal-mode representation over the Coleman-transform representation of the blade pitch has been added to the manuscript. Moreover, the discussion surrounding the clocking angle has been updated and it is clarified that the blade-pitch formulation is applied to each blade.

- Line 140, Table 1: I do not understand how the clocking angle creates a non-uniform thrust force across the rotor disk, as it is constant. If I understand correctly, the clocking angle is only relevant for the side-to-side and up-and-down strategies, in which case it is used to have the two modes negate each other in horizontal and vertical direction, respectively. For the other strategies, it only changes the phase of the excitation, which is why I do not understand why it is defined at 90 degrees. For the helix and pulse, the pitch angle can equivalently be written as (when $\phi_{clock} = 90$ degrees):

  $\Theta(t) = \Theta_0(t) - A\sin(\omega_e t - \kappa_\theta \psi(t))$

  Please clean up this definition.

  The reviewer is correct in that, for this study, the clocking angle, ϕ_{clock}, is mostly important for differentiating the side-to-side ($\phi_{\text{clock}} = 90°$) and up-and-down ($\phi_{\text{clock}} = 0°$) strategies. For the pulse and helix cases, the clocking angle is only relevant for the initial set-point of the blade pitch, and it is set to 90°. In situations with two-turbines, the clocking angle becomes important for the helix case (and other non-axisymmetric forcing strategies) when "synchronizing" wake control methods between upstream and downstream turbines [van Vondelen et al., 2025]; however, this is not the case here. The role of the clocking angle has been clarified in the manuscript.

- Line 199: Shouldn't it be $\hat{u}_j(r, \kappa_\theta, \omega)$ instead of θ?

  Yes, thank you for noticing this error. It has been update to $\hat{u}_j(r, \kappa_\theta, \omega)$.

- Figure 7: As mentioned before, this figure might not be necessary: A list/table of cross section locations would probably be clearer to me. Otherwise, the 3D representation does not seem to add much value to the figure and might even diminish clarity. Also, this paper uses normalized distance and centers around the turbine, whereas earlier figures used absolute distance. Please choose one or the other and apply throughout the paper (I would suggest using the one used here).

  The streamwise location of the planes in Figure 7 of the original manuscript have been added to the figure caption so that it is explicitly clear which cross section locations are used in the SPOD analysis.

- Figures 9 and 10: the panels in these figures are identical, but the subcaptions have very different sizes. Consider making these uniform.

  Thank you for pointing out this typesetting error. The subcaptions are consistent in the updated version of these figures (see Figures 4 and 5 in this document)

- Line 269: I can see how the swirl due to blade rotation can induce some contribution to the -1 mode, but I would expect it mostly influences this mode at the 1P frequency, not the St=0.3 frequency. Have you investigated this?

  → Line 270: Similarly, I can see how the veer contributes to the 1 mode, but would love to see a similar analysis in low-veer conditions to confirm this.

  → Line 405: I would indeed be very interested to see how the CW helix performs here, as you suggest. I would highly recommend adding this case to the paper. If the main contribution of this paper was to find the best AWM strategy for power extraction, it makes complete sense to ignore this case. However, as this paper is more about understanding the aerodynamics of AWM, I think adding this case to the paper would strengthen the findings.

  These three comments are excellent questions by the reviewer that the authors are hoping to address in a more thorough investigation in the future. Running additional LES cases is not permitted for this project at the moment, and repeating the analysis in this manuscript for a low-veer environment is outside of its scope. However, the effects of veer and swirl on active wake mixing strategies have been documented in other recent studies [Brown et al., 2025, Frederik et al., 2025, Coquelet et al., 2024], and the authors hope to extend the modal analysis developed in this paper to provide an explanation for the behavior observed in these studies soon.

- Figure 13: I'm not sure how much value this figure adds. Panel b looks very similar to 11a, as one would expect. Panel a shows that your SPOD is working, but does not really match the overall point you are trying to make in this section. Furthermore, it makes me question: do we not have the same leading blade-rotation defined SPOD modes at 0.1D downstream? I would expect so, but you do not show that.

  The reviewer is correct that Figure 13b looks similar to 11a in the original manuscript. This similarity arises because the blade pitch actuations induce a similar modal response in the induction field as in the near wake region at $St = 0.3$. However, unlike the near wake region, the dominant SPOD modes in the induction field do not occur at $St = 0.3$, but instead occur at the blade-passing frequency. This is not the case at $0.1D$ downstream, where the forced SPOD modes at $St = 0.3$ are dominant (Figure 11a in the original manuscript). The authors have decided to retain Figure 13 in the original manuscript to illustrate the difference (panel a) and similarity (panel b) between the modal structure of the induction field and the wake, and clarified this point in the manuscript.

- Line 345: I'm not sure I agree that the runoff is steep enough that you only need the first 1-2 SPOD modes to accurately represent the flow. If you want to make this claim, you should plot the flow according to the first 2 SPOD modes and compare it to the actual flow.

  The authors have revised the language regarding the eigenvalue decay in the near wake region for improved clarity. In the pulse and helix cases, an order-of-magnitude decrease in the eigenvalue spectrum is observed after the first three SPOD modes 0.5D downstream. In contrast, for the side-to-side and up-and-down cases, the decay is more gradual due to the forcing of two modes by the blade pitch actuations, resulting in an order-of-magnitude decrease after six SPOD modes.

- Figure 17: What does the tau in the subcaption of fig a mean?

  On line 360 of the original manuscript where the figure is first referenced, τ is defined as $\tau = \frac{1}{2\pi}\int_0^{2\pi} \mathcal{T}(r = D/2, \theta) d\theta$, i.e., it is a scalar measure of mean flow entrainment obtained by azimuthally averaging the radial shear stress flux around the circumference of a rotor disk. This has been clarified in the figure caption.

- Figures 16 and 18: consider making the limits of these figures a little smaller, as these figures show a lot of grey area that provide no information now.

  Thank you for this suggestion. The limits of Figures 16 and 18, as well as Figures 21 and 22, in the original manuscript have been adjusted, while maintaining the aspect ratio. For the reviewer's reference, the update version of Figure 16 is included below:

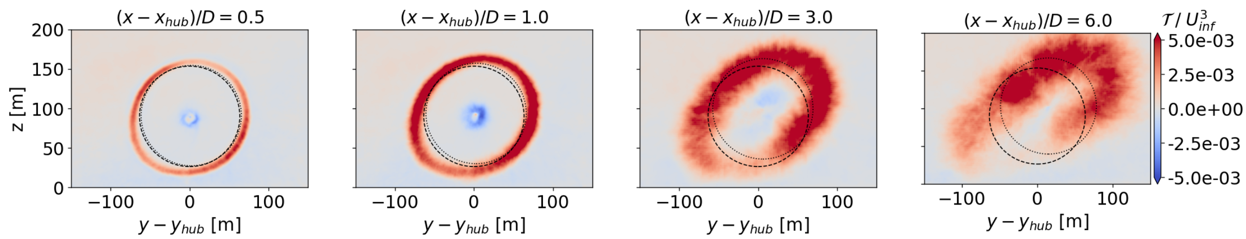

Figure 7: Contours of the radial shear stress flux for the baseline case at four different streamwise locations. The dashed line corresponds to the rotor disk centered at the hub height location and the dotted line corresponds to the rotor disk centered around the wake centers.

- Figure 20: Wouldn't it make more sense to plot —tau— here to make the figure smoother and more easily interpretable? Even if tau is negative, it still represents an eigenvalue, right?

  The quantity $\tau_{j,j}$ is not an eigenvalue; rather, it represents the contributions to the net radial shear stress flux from the jth SPOD mode. Specifically, $\tau_{j,j}$ is positive for any mode that leads to a net turbulent entrainment of mean velocity into the wake, and negative for modes leading to the entrainment of mean velocity out of the wake. The scalar $|\lambda_j|$ is the eigenvalue associated with the jth SPOD mode, and quantifies the turbulent kinetic energy associated with each mode. While it is possible to plot a monotonically decreasing $\tau_{j,j}$ spectra it would require a re-shuffling of the SPOD mode indices j (compare the top and bottom rows of Figure 8 in this document). Not only would this be confusing, but it would eliminate any sort of comparison between the energy contents of a mode and the mode's contribution to wake recovery. The SPOD formulation only guarantees a monotonic ordering of modes based on eigenvalues, and there is no reason to expect $\tau_{j,j}$ to line up with this ordering, especially for smaller turbulent scales. Throughout the manuscript, the modal index, j, is consistently ordered based on the SPOD eigenvalue, as is most natural, and $\tau_{j,j}$ is plotted with respect to this ordering. The authors have clarified the definition of $\tau_{j,j}$ in the manuscript and the intended purpose of Figure 20.

- Figures 21 and 22: if you want to keep these figures in the paper, you should include additional analysis of what you are showing here. It seems to me though that this analysis would not be in line with the main contribution of this paper, and is similar to previous LES studies performed on AWM. Furthermore, if you keep the figures, I would suggest using the same colormap throughout the paper (also applies to Fig 8).

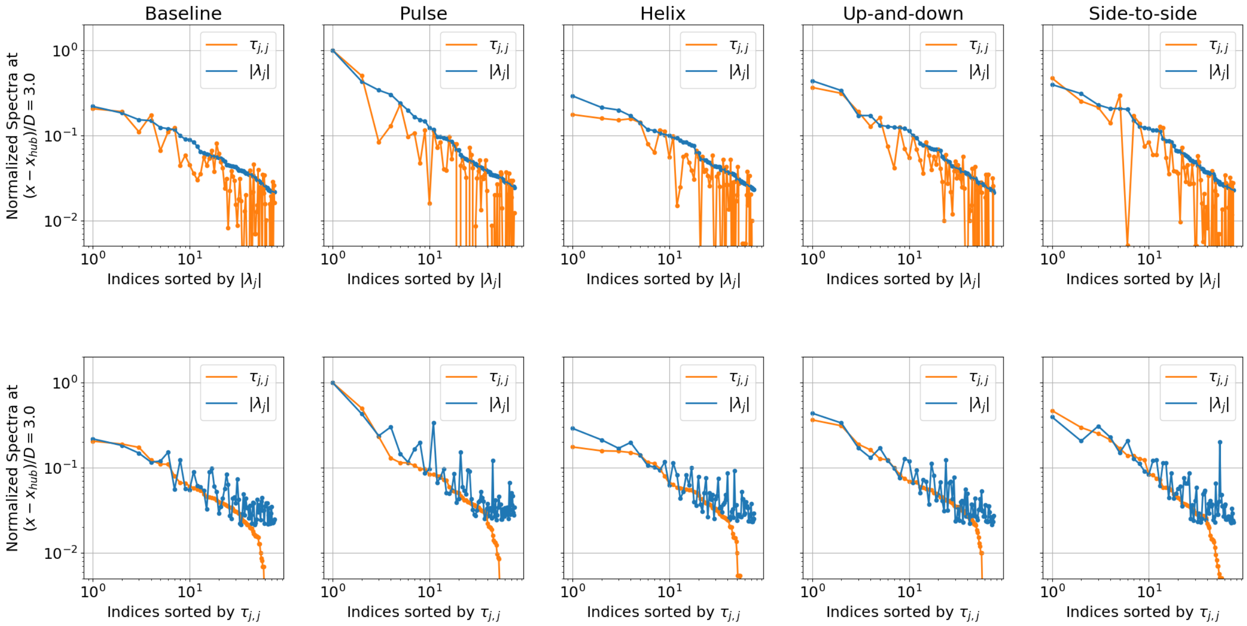

Figure 8: Energy and entrainment spectra defined by $|\lambda_j|$ and $\tau_{j,j}$, respectively, for the leading 75 eigenvalues at $(x - x_{hub})/D = 3$.

The authors have opted to retain Figures 21 and 22 in the manuscript and add additional text surrounding these figures. One of the main contributions of the paper is connecting the SPOD of the actuated flow to the wake recovery, including the mean velocity deficit and the radial shear stress flux. The authors feel the contour figures are particularly important to show in addition to the integrated values to demonstrate the anisotropy of these quantities around the rotor disk, especially compared to the canonical case (e.g., [Cheung et al., 2024]). This has been clarified in the manuscript.

The authors have ensured that the colormaps in the manuscript are consistent. For any *diverging* quantity, such as the radial shear stress flux, a red-blue color scheme is used. For any *sequential* quantity, such as streamwise velocity, a viridis color scheme is used.

- Line 435: Please show some verification (or refer to a paper that shows) that this approach yields reliable results. I understand that it is not feasible to run simulations at each downstream distance and for each case, but you could at least use say two cases to show how well this method estimates the power capture of an LES with 2 turbines. You might also want to add a description of this approach in Section 2.1.

  It is not feasible to run a two-turbine LES for this study; however, in lieu of this, it is common in the literature to estimate the power of a downstream turbine using the rotor averaged velocity (see, for example, [Taschner et al., 2024, Frederik et al., 2025]). As mentioned in an earlier response, we have chosen to approximate the power of the downstream turbine using an OpenFAST simulation coupled with inflow data from the LES from the appropriate location, instead of just approximating power based on rotor-averaged velocity. This should be more accurate than the rotor-averaged velocity approach as it includes the turbine model's response to the LES inflow data, instead of just the power coefficient. The OpenFAST simulation also provides a measurement of the loads on the downstream turbine, which is an important consideration for wake control methods that cannot be evaluated from rotor-averaged velocity alone. The authors would characterize the approach as a good compromise between conducting a full LES and simply analyzing rotor-averaged velocities.

- Figure 23: consider adding in some way the results from Figure 17 in Figure 23 to make it easier for the reader to verify how well the rotor averaged velocity predicts downstream power. For this purpose, you might need to plot just the downstream power separately. Also, there seems to be a very thin grey line around this figure, is that done on purpose?

  The authors have included the results for the downstream turbine's power in the updated version of this figure (see Figure 6 in this document). The rotor-averaged velocities are presented in a separate figure due to the slight vertical shift in the wake which the downstream turbine cannot follow; however, the trends are closely aligned. The authors appreciate the reviewer's suggestion and have also removed the mysterious thin grey line.

- Figure 24: If you do keep this figure, it makes no sense to me to unify the y-axes like you did here. The top 4 panels now provide close to no information as the differences are indistinguishably small. But similar to my main comment about Figure 23, I do not think this analysis adds much value to the paper and perhaps should be cut altogether.

  Figure 24 of the original manuscript has been revised so that the y-axes are no longer unified across load channels (see Figure 9 in this document). Please note that some of the additional white space in the figures arises from the values of the DLC 1.2 case, which provides important context for the baseline loads.

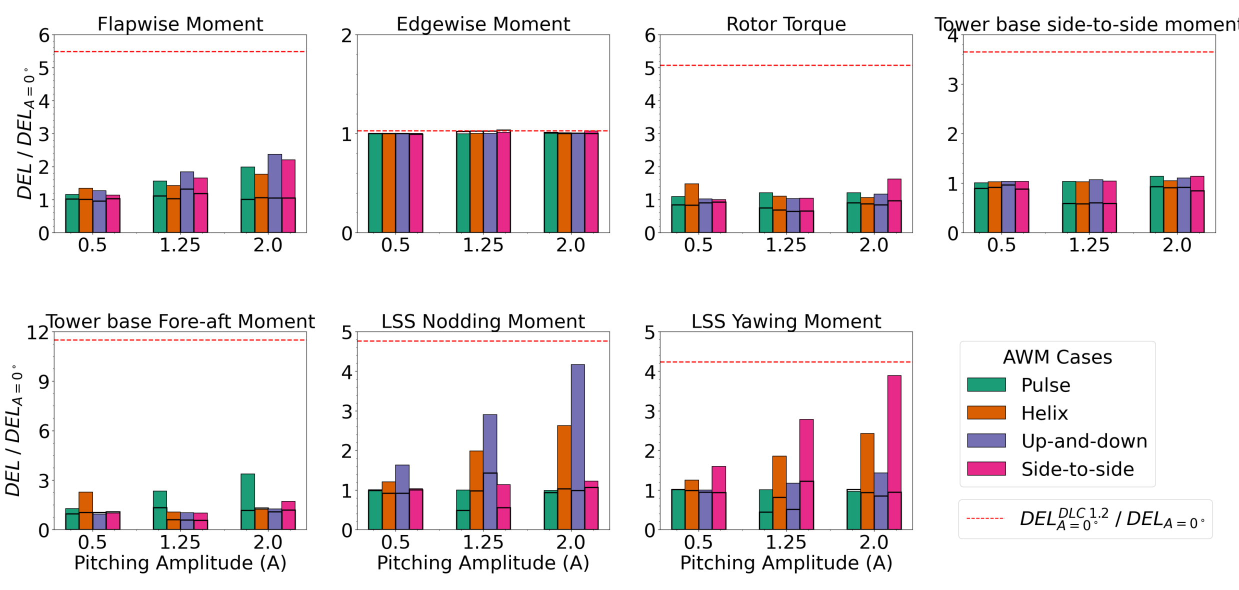

Figure 9: Baseline-normalized damage equivalent loads (DEL) for seven different load channels at three different pitching amplitudes, $A = 0.5°$, $A = 1.25°$, and $A = 2.0°$. Solid bars indicate DELs for the upstream turbine, while the DELs for the turbine $6D$ downstream are outlined in black. The red dashed line corresponds to the baseline-normalized DELs from a normal turbulence model in a DLC 1.2-like environment (single seed) with a hub height wind speed of 6.4 m/s, a shear exponent of 0.12, and a turbulence intensity of 25.90%.

References

Kenneth Brown, Gopal Yalla, Lawrence Cheung, Joeri Frederik, Nate deVelder, Dan Houck, Eric Simley, and Paul Fleming. Comparison of wind farm control strategies under a range of realistic wind conditions: wake quantities of interest. Wind Energy Science, 2025.

Lawrence C Cheung, Kenneth A Brown, Daniel R Houck, and Nathaniel B deVelder. Fluid-dynamic mechanisms underlying wind turbine wake control with strouhal-timed actuation. Energies, 17 (4):865, 2024.

M Coquelet, J Gutknecht, JW Van Wingerden, M Duponcheel, and P Chatelain. Dynamic individual pitch control for wake mitigation: Why does the helix handedness in the wake matter? In Journal of Physics: Conference Series, volume 2767, page 092084. IOP Publishing, 2024.

Joeri Frederik, Eric Simley, Kenneth Brown, Gopal Yalla, Lawrence Cheung, and Paul Fleming. Comparison of wind farm control strategies under a range of realistic wind conditions: turbine quantities of interest. Wind Energy Science, 2025.

E Taschner, M Becker, Remco Verzijlbergh, and JW Van Wingerden. Comparison of helix and wake steering control for varying turbine spacing and wind direction. In Journal of Physics: Conference Series, volume 2767, page 032023. IOP Publishing, 2024.

Aemilius Adrianus Wilhelmus van Vondelen, Marion Coquelet, Sachin Tejwant Navalkar, and Jan-Willem van Wingerden. Synchronized helix wake mixing control. Wind Energy Science Discussions, 2025:1–36, 2025.